ANL/PHY/CP--91683 CONF-9607177--1

NUCLEON SPIN STRUCTURE FUNCTIONS FROM HERMES-THE FIRST YEAR

H. E. Jackson

Argonne National Laboratory, Argonne. Il. 60439

On Behalf of the HERMES Collaboration

Abstract

HERMES, HERA Measurement of Spin, is a second generation experiment to study the spin structure of the nucleon by using polarized internal gas targets in the HERA 28 GeV electron storage ring. Scattered positrons and coincident hadrons are detected in an open geometry spectrometer which includes particle identification. Inclusive data with polarized ^{3}He give the spin structure function $g_1^n(x)$ and the Ellis-Jaffe integral $\Gamma_1^n = \int_0^1 g_1^n(x)dx$ for the neutron. The semi-inclusive spin asymmetries are a unique and sensitive probe of the flavor dependence of quark helicity distributions and properties of the quark sea. Data taken in 1995 with unpolarized hydrogen and deuterium targets provide measurements of the flavor distributions of sea and valence quarks. In a preliminary analysis, $\Gamma_1^n = -0.032 \pm 0.013_{stat.} \pm 0.017_{syst.}$ is obtained at $Q^2 = 3(GeV/c)^2$ for the Ellis-Jaffe integral.

I. INTRODUCTION

The spin structure of the nucleon continues to be a topic of intense interest, in spite of many years of experimental study[1-3]. To date, emphasis has been placed on the determination of the "Ellis-Jaffe integrals", i.e. the first moments of the $g_1(x)$ spin structure function

DISCLAIMER

of the nucleon. Here $x = Q^2/2m\nu$ is the usual Bjorken scaling variable. The conclusions of these polarized deep-inelastic scattering experiments has been that $\sim 30\%$ of the proton's spin is carried by the quarks[4], much less than that predicted by "naive" models of nucleon spin structure. More detailed issues, such as the polarization of the sea and the glue, remain largely inaccessible to experiment. HERMES is a second generation experiment[5] designed to study the spin structure of the nucleon in a level of detail not possible in earlier measurements by using the electron storage ring of the HERA accelerator. Measurements of inclusive cross sections are possible from undiluted targets of hydrogen, deuterium, and ^{3}He for any target polarization state. Semi-inclusive spin asymmetries resulting from hadron particle identification provide a means of selecting quark flavors by tagging leading hadrons. The first year of operations was completed recently. The first results from the analysis of the data accumulated in 1995 is presented here.

II. PHYSICS OF SPIN ASYMMETRIES

The basic features of the scattering of polarized leptons by polarized nucleons are determined by the spin structure functions, $g_1(x)$ and $g_2(x)$. From recent data, it has been established[6] that $g_2(x)$ is small. Consequently, the scattering of longitudinally polarized leptons by longitudinally polarized nucleons can be described sufficiently accurately[7] by $g_1(x)$ alone. Here $g_1(x)$ is extracted from the virtual photon asymmetry, $A_1(x)$, generated by the scattering of polarized electrons. The experimentally measured electron asymmetry, $A_e(x)$, is related to $A_1(x)$ by a depolarization parameter, $D(x,y)$:

$$A_e(x) = \frac{\sigma(e)_{\uparrow\downarrow} - \sigma(e)_{\downarrow\downarrow}}{\sigma(e)_{\uparrow\downarrow} + \sigma(e)_{\downarrow\downarrow}} \approx D(x,y)A_1(x)\,; \;\; D(x,y) = \frac{y(2-y)}{y^2 + 2(1-y)[1+R(x,y)]}. \qquad (1)$$

$R(x,y)$ is the ratio of cross sections for longitudinally and transversely polarized virtual photons. To a good approximation $A_e(x) \approx g_1(x)D(x,y)/F_1(x)$. From the electron asymmetry one deduces $g_1(x)$, which to lowest order, in the Quark Parton Model is

$$g_1(x) = \frac{1}{2}\sum_{i=1}^{n} e_i^2[q_i^{\uparrow}(x) - q_i^{\downarrow}(x)]. \qquad (2)$$

The quark distribution functions, $q_i^{\uparrow(\downarrow)}(x)$, refer to quarks with spin parallel(antiparallel) to the nucleon spin.

In the naive parton model, the first moment of $g_1(x)$ provides one constraint on the flavor dependence of the net quark helicities, $\Delta q_i = \int_0^1 [q_i^{\uparrow}(x) - q_i^{\downarrow}(x)]dx$:

$$\int_0^1 g_1^p(x)dx = \frac{1}{2}(\frac{4}{9}\Delta u + \frac{1}{9}\Delta d + \frac{1}{9}\Delta s)(1 - O(\alpha_s)). \tag{3}$$

Constraints on the Δq_i's also come from applying isospin and SU(3) flavor symmetries[8] to neutron decay and semi-leptonic hyperon decay data:

$$\Delta u - \Delta d = F + D \; ; \; \Delta u + \Delta d - 2\Delta s = 3F - D. \tag{4}$$

where F and D are the renormalization constants of the standard SU(3) matrix elements. If one assumes in addition to SU(3) symmetry, that the strange sea is unpolarized[9], the matrix elements for neutron and hyperon decay alone fix the total quark spin in the nucleon, $\Delta u + \Delta d + \Delta s$, at the value of ≈ 0.6, the "canonical expectation." However, as noted above, experimental data indicate a value of only ≈ 0.3. The Bjorken sum rule[10], a fundamental relationship arising from current algebra between the difference in the first moments of the proton and the neutron is confirmed by the data, but the Ellis-Jaffe sum rule[9] which also follows from SU(3) symmetry and the assumption that the strange sea is unpolarized is violated. Thus, in spite of careful and extensive efforts, the formulation of a model of nucleon spin structure, which accounts for all the spin in terms of the partonic constituents remains a clear challenge.

Semi-inclusive hadron asymmetries contain additional information which can be of great value in the studies of the flavor dependence of quark helicity distributions in the nucleon, and of the contributions of the valence and sea quarks to the total nucleon polarization. The spin asymmetry for polarized π^- electroproduction is an excellent example. In the parton picture, because of the dominance of the $\bar{u}$ channel in fragmentation to $\pi^-(\bar{u}d)$, the π^- asymmetry should be very sensitive to the sea polarization. For scattering from a longitudinally polarized proton target, the π^- asymmetry is

$$A_p^{\pi^-} = \frac{\pi^-_{\uparrow\downarrow} - \pi^-_{\downarrow\downarrow}}{\pi^-_{\uparrow\downarrow} + \pi^-_{\downarrow\downarrow}}. \tag{5}$$

Application of the standard parton model with the assumptions of charge conjugation and isospin invariance of the of the quark fragmentation functions[11,12] gives the following form for $A_p^{\pi^-}$

$$A_p^{\pi^-} = \frac{4\Delta u^v + \eta\Delta d^v + 5(1+\eta)\Delta\bar{q} + 2\Delta s}{4u^v + \eta d^v + 5(1+\eta)\bar{q} + 2s}. \tag{6}$$

Here Δu^v,Δd^v are the polarized valence quark distributions, $\Delta\bar{q}$ indicates the polarized sea with$\Delta u_s = \Delta\bar{u}_s = \Delta d_s = \Delta\bar{d}_s$, Δs is the polarized strange quark distribution, u^v,d^v,$\bar{q}$, and s are the analogous unpolarized counterparts. The ratio, η, of favored (struck quark) to unfavored fragmentation functions,

$$D(z) = \eta\tilde{D}(z)\,; \;\; \eta \approx \frac{1+z}{1-z} \tag{7}$$

where η has the form originally suggested by Feynman and Field[13] and confirmed by the EMC collaboration[14]. $A_p^{\pi^-}$ contains contributions from both valence and sea quarks. The valence contribution is small because of cancellation between the contributions of the u^v and d^v terms. At small x, where the sea dominates, a substantial sea polarization will generate large observable π^- asymmetries.

In HERMES, both inclusive and semi- inclusive spin asymmetries are measured. The experiment runs at the HERA beam energy of 27.5 GeV with an angular acceptance of $40 < \theta < 220$ $mrad$. The kinematic range accessible is $0.02 < x < 0.8$ and $0.2 < Q^2 < 20$ $(GeV/c)^2$. The targets can be hydrogen, deuterium, or ^{3}He in any polarization state, including in the case of the deuteron a tensor-polarized state. Inclusive measurements are currently focused on the determination of $g_1(x)$ for the neutron and proton. Unambiguous identification of pions with a threshold Cerenkov counter provides the first direct measurement of semi-inclusive spin asymmetries. The results, shown in Fig. 1, of a Monte Carlo simulation using recently compiled parton distributions[15] demonstrate that the measurement of $A_p^{\pi^-}(z)$ can provide a clear, simple, and precise determination of the nonstrange sea polarization.

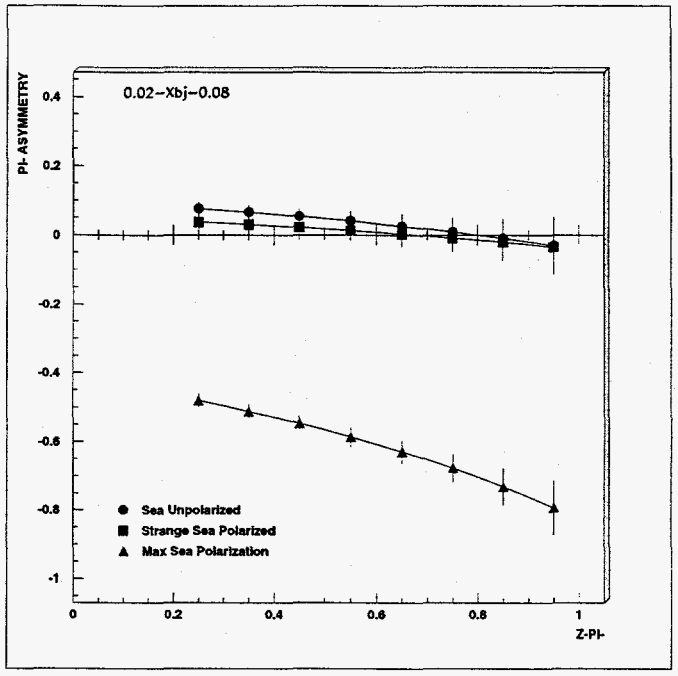

FIG. 1. Results of a HMC Monte Carlo simulation of $A_p^{\pi^-}(z)$ for an unpolarized sea, for a maximally negatively polarized strange sea, $(\Delta\overline{q} = 0.0, \Delta\overline{s} = -\overline{s})$, and for a totally negatively polarized sea with $0.02 \geq x_{bj} \geq 0.08$. The error bars indicate the statistical precision with which $A_p^{\pi^-}$ would be measured in a $600hr$ run.

The valence contribution is small as evidenced by the small value of $A_p^{\pi^-}(z)$ for a non-polarized sea. For π^+ electroproduction, the valence contribution gives $A_p^{\pi^+}(z) \approx 0.2$ for a non-polarized sea, making the observation of small sea contributions more difficult.

III. THE EXPERIMENT

The internal polarized ^3He gas target for HERMES is shown schematically in Fig. 2. It consists of an open-ended thin walled storage cell through which the circulating positron beam of the HERA accelerator passes. The figure shows the cell as filled with

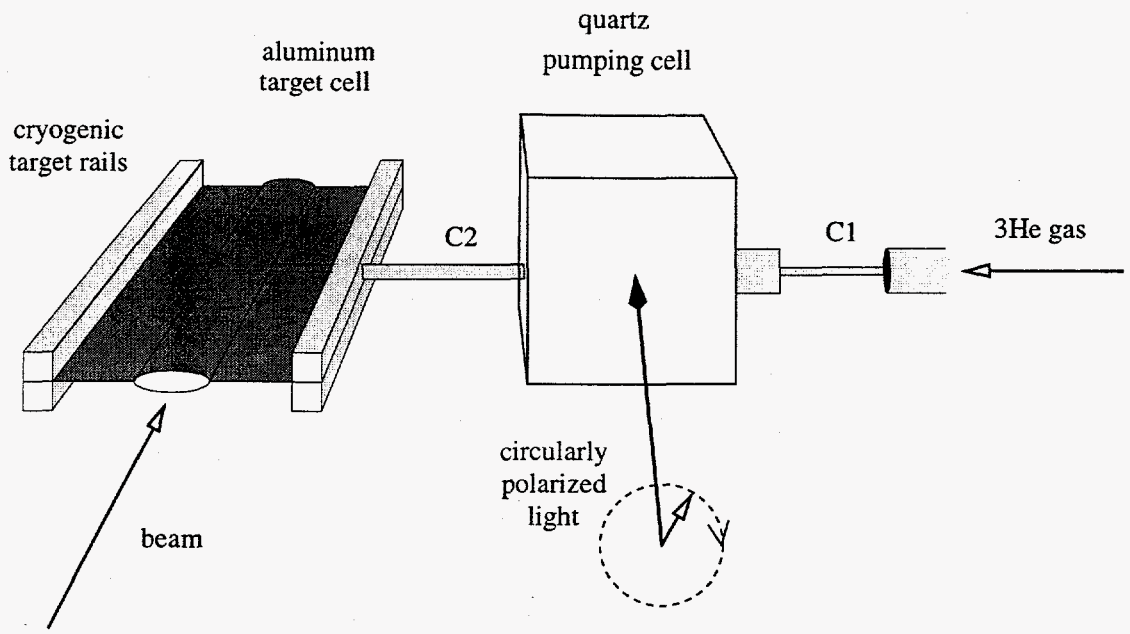

FIG. 2. Schematic view of the polarized ^3He target with the gas inlet at the right, the density regulating conductance C1 and the pumping cell. From the pumping cell the polarized gas enters the cell through C2.

^3He from an optically pumped source. It can also be filled with polarized protons or deuterons from an atomic beam source. A solenoidal holding field provides a quantization axis for the target polarization. The target densities are about $10^{14} atoms/cm^2$ for hydrogen and deuterium and $3.5 \times 10^{14} atoms/cm^2$ for ^3He. Luminosities are in the range of $4 - 30 \times 10^{31} nucleons\, cm^{-2} sec^{-1}$.

The gases are pure so that there is no target dilution. The extremely small target thickness minimizes external radiative corrections. During the 1995 running, a longitudinally polarized ^{3}He target was used. The average target polarization was 0.475. The spin orientation was reversed every 10 minutes. In addition, measurements were carried out with unpolarized targets of hydrogen and deuterium. For these measurements, the storage cell was filled with molecular hydrogen and deuterium at a densities in the range $.6 - 1.0 \times 10^{15} atoms/cm^2$.

The experiment is located in the east Hall of the HERA accelerator where the interaction area is configured so that the proton beam bypasses the HERMES target. The beam is

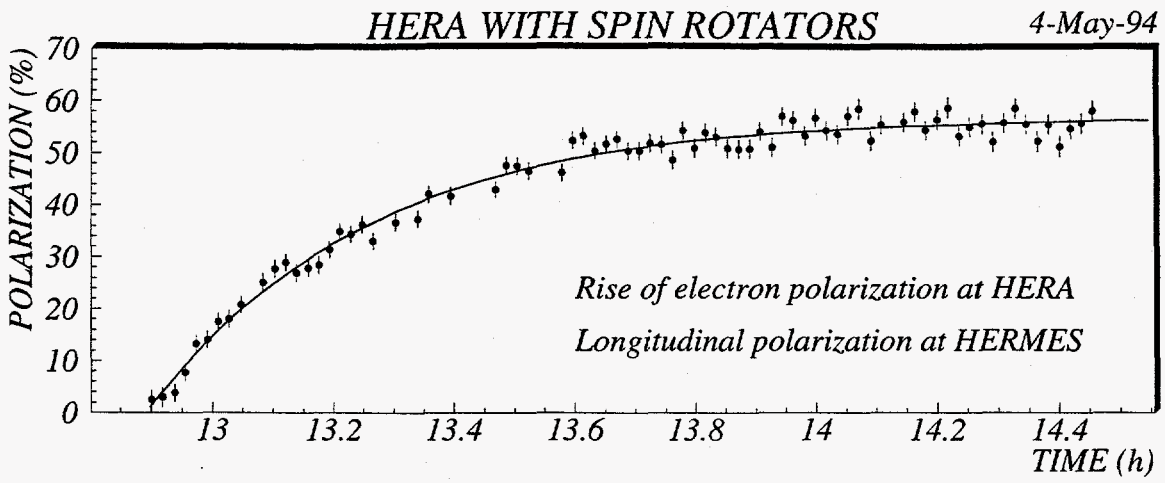

FIG. 3. t' distribution $N_N(t')$ for a pure sample of non-exclusive $^3\mathrm{He}(e,e'h^+h^-)$ events (left plot) and the distribution $N_{S+N}(t')$ for a mixed sample of exclusive and non-exclusive events (right plot). The solid lines are fits using one (left plot) or two (right plot) logarithmic slope parameters, and the short-dashed line is an extrapolation beyond the fit region. The long-dashed line in the right plot represents the incoherent contribution. Also shown (dot-dashed line) is the inferred non-exclusive contamination $f_{\Delta E,\mathrm{sub}}N_N(t')$ of the right plot.

polarized transverse to the beam direction by the Sokolov-Ternov effect[16]. In a perfect machine it will reach 92%. Spin rotators located at the entrance and exit of the hall[17] precess the spin direction from vertical to longitudinal at the target position and, following the target, back to the vertical position. The polarization of the beam with the rotators in place has been measured for both positrons and electrons. The results of a typical measurement are shown in Fig. 3. Longitudinal polarizations of about 60% are stable and reproducible. The polarization time is about 20 minutes.

As a result of the ease with which the direction of the target polarization can be changed, it will be possible to study parallel and perpendicular polarization asymmetries for all targets. In addition to measurements of $g_1(x)$ and $g_2(x)$, and the Bjorken sum rule, estimates

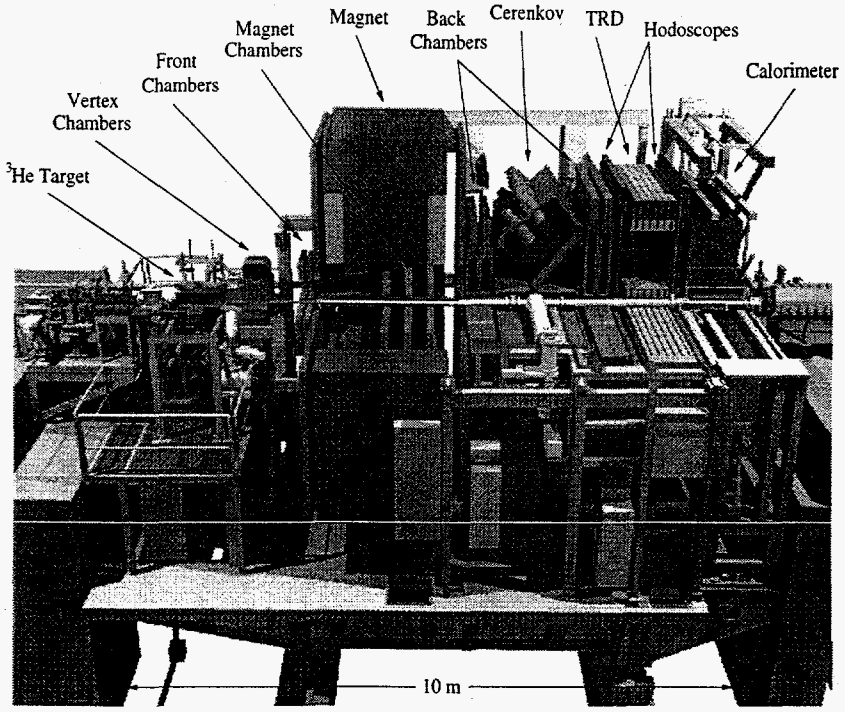

FIG. 4. Schematic view of the HERMES spectrometer. A median plane magnet flux plate, with the positron and the proton beam pipes divide the detector system into upper and lower identical sections.

will be made of the higher order structure functions $b_1(x)$[18] and $\Delta(x)$[19] which are relevant to the deuteron.

The HERMES spectrometer, shown in Fig. 4, is an open geometry system. A magnet with a bending strength of 1.3 T-m is used to measure particle momenta. The magnet is divided into 2 symmetric parts by a horizontal flux plate through which both the electron and proton beam pass.

A system of segmented hodoscopes and a fly's eye lead glass calorimeter provide a deep inelastic scattering trigger. A transition radiation detector(TRD) provides strong discrimination against pions. Tracking chambers before the magnet, in the magnetic field, and behind the magnet provide charged particle tracking. A pair of threshold gas Cerenkov counters are used for identification of hadrons. Each Cerenkov unit is divided into 20 cells

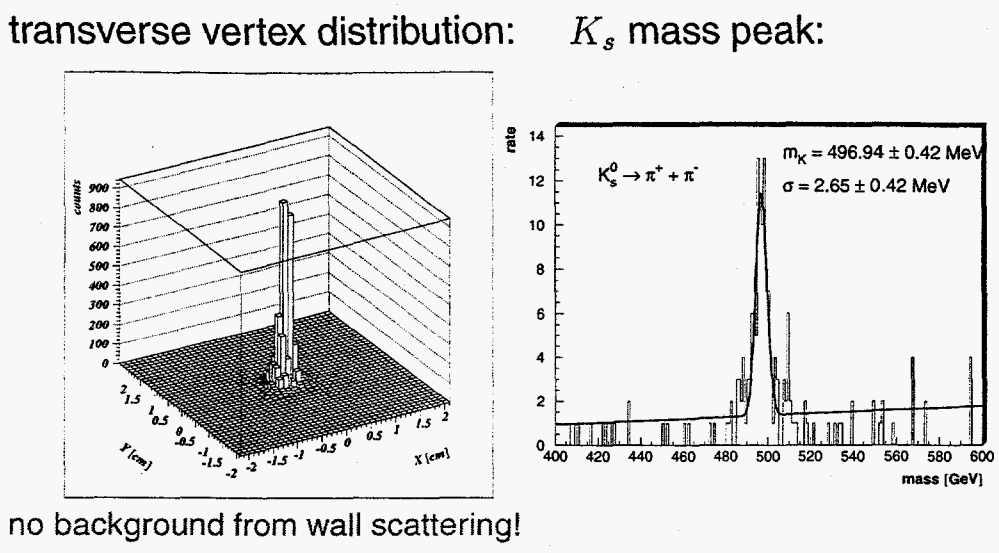

FIG. 5. Data from Event Reconstruction. The section at the left shows the transverse vertex distribution for deep ineleastic scattering events. The section at the right shows a reconstructed K^0_s invariant mass spectrum obtained from the H_2/D_2 data.

viewed by individual photomultipliers. Relative luminosity is monitored with $\approx 1\%$ precision by the coincident detection in symmetrically placed bismuth tungstenate calorimeters of the positron-electron pair from symmetric Bhabha scattering off the target atomic electrons. The target empty luminosity rate is negligible.

IV. SPECTROMETER PERFORMANCE AND PARTICLE YIELDS

A measure of the performance of the HERMES spectrometer is provided by the data presented in Fig. 5. At the right the invariant mass peak is shown which from $^3He(e, e'h^+h^-)$ assuming the hadrons are pions. A cut has been applied on the distance between the target vertex and the K^0_s decay vertex to reduce the combinatorial background. A K^0_s peak is observed with a missing mass resolution of 2.65 MeV.

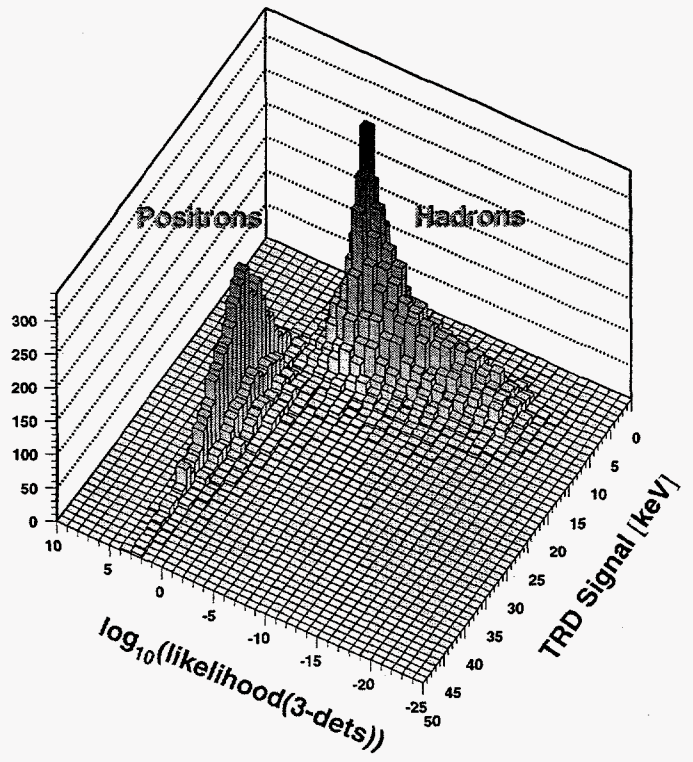

FIG. 6. TRD signal versus a three detector particle identification likelihood function calculated from the response of the preshower counter, calorimeter, and Cerenkov counter.

At the left, the transverse vertex distribution is shown. No background scattering is observed from the target walls. Particle identification in HERMES is provided by the response of four detector systems: a preshower section, the calorimeter, the TRD, and the Cerenkov counter. Fig. 6 shows the clean separation of hadrons and positrons which results from plotting the TRD signal against a particle identification likelihood function calculated from the response of the other three detectors. Pions can be separated from other hadrons between the pion and kaon threshold momenta for radiation in the Cerenkov counter.

The approximate particle yields obtained during the 1995 running are presented in Table 1. In addition to copious numbers of pions, a clean peak of ρ^0's has been reconstructed from the data. Substantial numbers of kaons and lambda's are observed, and although precise numbers are not available, there appear to be J/Ψ and open charm events at the level of a

TABLE I. Approximate hadron yields from 5.8 million deep-inelastic scattering events on longitudinally polarized ^3He.

Particle	Approx. Yield	Particle	Approx. Yield
π^0	100k	ρ^0	9k
π^+	330k	P	~16k
π^-	220k	$\bar{P}$	~1500
K^+	~5k	Λ	~1000
K^-	~6k	J/Ψ	~40-100
K_s^0	900	$D^0, \bar{D}^0$	~100?

few hundred.

The kinematic region covered by HERMES for a beam energy of 27.5 GeV is shown in Fig. 7. Several kinematic cuts are shown. A minimum momentum transfer (not shown) of $Q^2 \geq 1.0\ GeV^2$ facilitates interpretation of the data in terms of the quark parton model. A cut on the invariant mass of $W^2 \geq 6\ GeV^2$ eliminates contributions from the resonance region.

A cut on the energy loss of $y \leq 0.85$ eliminates large radiative corrections. With these cuts measurements can be made over the range $0.02 < x_{bj} < 0.8$

V. RESULTS

A limited amount of data was taken in 1995 with unpolarized hydrogen and deuterium targets to establish the reliability and precision of the HERMES spectrometer. A number of interesting topical physics problems can be studied with this data. One important quantity, the structure function ratio F_2^n/F_2^p of the neutron and proton can be measured directly from the ratio of the DIS yields for the proton and the deuteron. Instrumental efficiencies and acceptances cancel to first order. Only corrections for kinematic smearing, radiation, and nuclear binding effects need be considered. Fig. 8 shows the results of an analysis[20] of 43

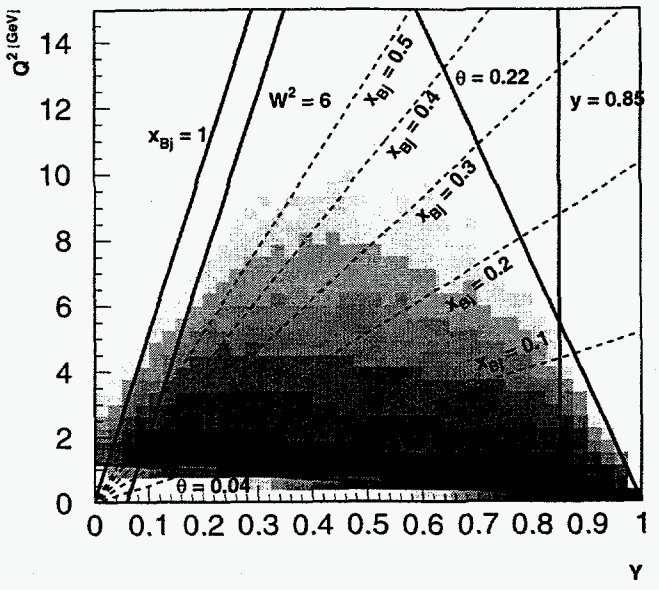

FIG. 7. Kinematic cuts in the $Q^2 - y$ plane. The angular acceptance of the HERMES spectrometer is between the solid lines labeled $\theta = 0.04$ *and* 0.22 *mr*. The shaded area shows the distribution of reconstructed events.

hours of data.

The results agree well with measurements from NMC[21] and SLAC[22].

A second interesting quantity accessible in the unpolarized data is the valence quark ratio, $d_v(x)/u_v(x)$, for the proton. Because the leading hadrons in fragmentation contain the struck quark, the pion multiplicities are sensitive to the quark flavor distributions. The ratio, $d_v(x)/u_v(x)$ can be estimated from the experimentally measured pion ratio, $R_\pi(x)$:

$$R_\pi(x) = \frac{N^{d\pi^+}(x) - N^{d\pi^-}(x)}{N^{p\pi^+}(x) - N^{p\pi^-}(x)} \cdot \frac{N^p(x)}{N^d(x)} \cdot (1 + \frac{F_2^n(x)}{F_2^p(x)}) - 1. \tag{8}$$

The ratio of quark distributions can be calculated directly from $R_\pi(x)$:

$$\frac{d_v(x)}{u_v(x)} = \frac{4R_\pi(x) + 1}{R_\pi(x) + 4} \tag{9}$$

The results obtained for this ratio are presented in Fig. 9 for two analyses. In one, the mea-

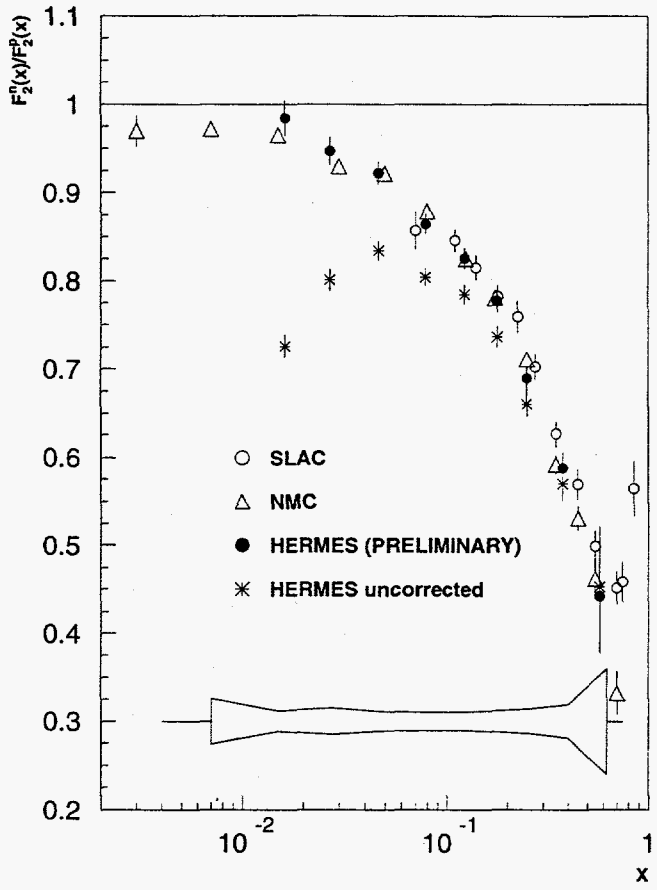

FIG. 8. The ratio $F_2^n(x)/F_2^p(x)$ vs x measured in HERMES95 compared with previous measurements at CERN and SLAC. The radiatively corrected data are shown as solid dots, for comparison the uncorrected data are shown as stars. The gray area gives an upper bound for the systematic uncertainties.

sured ratios result from an analysis using all hadrons and correcting[23] for the contamination of the pion sample by kaons and nucleons.

In the second, only identified pions are used. The agreement with earlier experiments is excellent. With the improved particle identification expected in 1996, HERMES will provide new information on this ratio.

A preliminary analysis of the data taken with a polarized ^3He target has been carried out in order to extract the spin structure function $g_1^n(x)$. The inclusive spin asymmetries were extracted from the scattered positron yields using the luminosity monitor for relative normalization. Radiative corrections were made by means of the techniques of Akushevich and Shumeiko[24]. Instrumental smearing was confirmed to be small. Pending a more complete understanding of spectrometer instrumental effects and unresolved issues of analysis procedures, points at lowest and highest x_{bj} were excluded from the results reported here. Stringent quality cuts eliminated from analysis over half of the $\approx$ 5.8 million events accumulated. The preliminary results for g_1^n are presented in Fig. 10. Only statistical errors are shown. The results are in good agreement with the data reported from SLAC experiment E-142[1] also using a ^3He target.

The Ellis-Jaffe integral $\Gamma_1^n = \int_0^1 g_1^n(x)dx$ can be estimated from the data on $g_n^1(x)$ by evolving the points to a fixed value of $Q^2 = 3\ (GeV/c)^2$ assuming that the measured asymmetry $A_1^n(x)$ is independent of Q^2. Simple models employed in the analyses of previous experiments have been used to extrapolate $g_n^1(x)$ outside the measured region, giving $g_n^1(x)$ =const for $x < 0.03$[25] and $g_n^1(x) \approx (1-x)^3$ for $x > 0.6$[26]. With these extrapolations, the integral of $g_1^n(x)_{measured}$ is

$$\Gamma_1^n = -0.032 \pm 0.013_{stat.} \pm 0.017_{syst.} \tag{10}$$

The relatively large statistical and systematic errors reflect the preliminary character of the analysis. A comparison of the HERMES result with those of all recent measurements is shown in Fig. 11.

Within the errors cited, the results of all experiments reported are in agreement. The

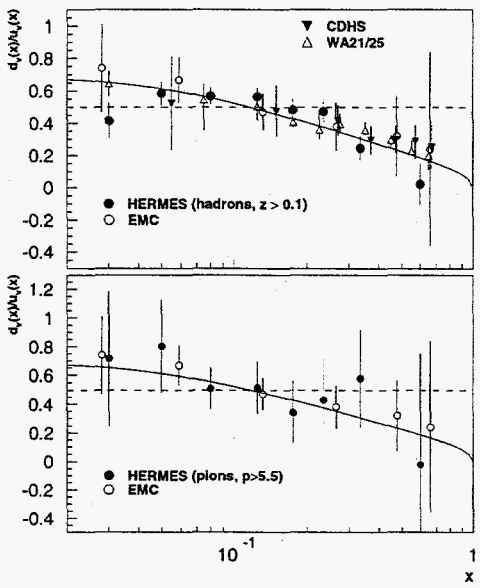

FIG. 9. The valence quark distribution function ratio (statistical errors only for HERMES95, for WA21/25, EMC and CDHS stat. and sys. combined). The upper plot shows the HERMES95 and EMC result using all hadrons. The triangles are measurements from neutrino/anti-neutrino experiments. The line is the CTEQ3M parameterization for the valence quark distribution functions. The lower plot shows the same EMC data and a CTEQ fit but with HERMES95 data using the pion PID, in which case the correction for the hadron fragmentation functions is not needed. The dashed lines indicate the naive QPM expectation with exact SU(6) symmetry.

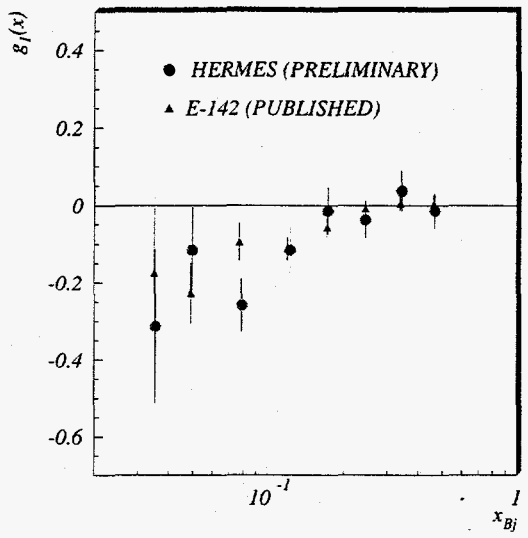

FIG. 10. The preliminary result for the spin structure function $g_1^n(x)$ obtained from the inclusive spin asymmetry on ^3He measured in HERMES95. Also shown are the data from SLAC measurement E-142.

various data bands intersect in a region consistent with the Bjorken sum rule and violate the Ellis-Jaffe sum rule at the level of 2σ.

VI. CONCLUSIONS

The HERMES experiment started data acquisition in 1995. Luminosity and polarization are high, and backgrounds are low. Unpolarized structure function and charged pion multiplicity ratios have been extracted from data with unpolarized targets and agree with the world data base. The preliminary result for g_1^n obtained with polarized ^3He is consistent with data from earlier experiments. High yields of a range of hadrons demonstrate the opportunity to pursue flavor tagging by measurement of specific semi-inclusive cross sections.

Acknowledgements

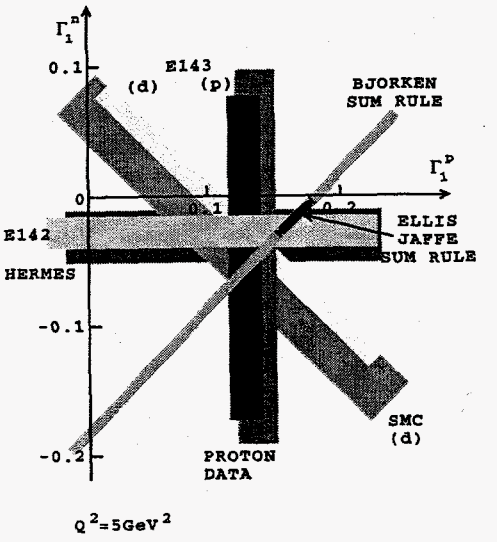

FIG. 11. Summary of all recent measurements for the Ellis-Jaffe integrals Γ_1^p and Γ_1^n at $Q^2 = 5GeV^2$. Also shown are the regions allowed by the Bjorken and Ellis-Jaffe sum rules.

This work is supported in part by the U.S. Department of Energy, Nuclear Physics Division under contract W-31-109-ENG-38.

REFERENCES

[1] D. L. Anthony et al., Phys. Rev. Lett. **71**, 959 (1993).

[2] B. Adeva et al., Phys. Lett. **B320**, 400 (1994); D. Adams et al.,Phys. Lett. **B329**, 399 (1994).

[3] K. Abe et al., Phys. Rev. Lett **74**, 346 (1995).

[4] J. Ellis and M. Karliner, Phys. Lett. **B341**, 397 (1995).

[5] HERMES collaboration, *Technical Design Report*, DESY-PRC 93/06 (1993).

[6] B. Adams et al., Phys. Lett. **B336**, 125 (1994).

[7] For a more complete treatment including effects of $g_2(x)$ see H. E. Jackson in: *AIP Conference Proceedings 343*, Proceedings of the 11th International Symposium on High Energy Spin Physics, ed. by K. Heller and S. Smith (American Institute of Physics, Woodbury, N. Y. 1995).

[8] R. L. Jaffe and A. Manohar, Nucl. Phys. **B337**, 509, (1990).

[9] J. Ellis and R. J. Jaffe, Phys. Rev. **D9**, 1444 (1974).

[10] J. Bjorken, Phys. Rev. **148**, 1467 (1966); **D10** 1376 (1970).

[11] L. L. Frankfurt et al., Phys. Lett. **B230**, 141 (1989).

[12] F. E. Close and R. G. Milner, Phys. Rev. **D44**, 3691 (1991).

[13] R. D. Field and R. P. Feynman, Phys. Rev. **D15**, 2590 (1977).

[14] J. J. Aubert et al., Phys. Lett. **B160**, 417 (1985).

[15] H. E. Jackson, HERMES Internal Note **95-031**, 1995.

[16] A. A. Sokolov and I. M. Ternov, Sov. Phys. Doklady **8**, 1203 (1964).

[17] J. Buon and K. Steffen, Nucl. Instr. Methods **A245**, 248 (1986).

[18] P. Hoodbhoy, R. L. Jaffe, and A. Manohar, Nucl. Phys. **B312**, 571 (1989).

[19] R. L. Jaffe and A. Manohar, Phys. Lett. **B223**, 218 (1989).

[20] K. Ackerstaff, PhD thesis, Univ. Hamburg (1996).

[21] P. Amaudruz et al., Nucl. Phys. **B371**, 3 (1992).

[22] L. W. Whitlow et al., Phys. Lett. **B282**, 475 (1992).

[23] J. Ashman et al., *Forward produced hadrons in μp and μd scattering and investigation of the charge structure of the nucleon*, CERN-PPE/91-53, March (1991).

[24] I. V. Akushevich and N. M. Shumeiko, J. Phys. G: Nucl. Part. Phys. **20**, 513 (1994).

[25] J. Ellis and M. Karliner, Phys. Lett. **B213**, 73 (1988).

[26] S. J. Brodsky et al., Nucl. Phys. **B441**, 197 (1995).